Supporting information

Benzimidazole-dioxoisoindoline conjugates as dual VEGFR-2 and FGFR-1 inhibitors: design, synthesis, biological investigation, molecular docking studies and ADME predictions

Heba T. Abdel-Mohsen,[1]* Amira M. Nageeb[2]

[1]Chemistry of Natural and Microbial Products Department, Pharmaceutical and Drug Industries Research Institute, National Research Centre, Dokki, P.O. 12622, Cairo, Egypt.

[2]High Throughput Molecular and Genetic Technology Lab, Center of Excellence for Advanced Sciences, Biochemistry Department, Biotechnology Research Institute, National Research Centre, Dokki, P.O. 12622, Cairo, Egypt.

*Corresponding author. Email address: ht.abdel-mohsen@nrc.sci.eg and hebabdelmohsen@gmail.com (Heba T. Abdel-Mohsen)

Contents **Page**

1.	**NMR Spectra of target benzimidazole-dioxo(benzo)isoindoline hybrids 8a-o**	**2**
2.	**HRMS spectra of 8c and 8m**	**17**
3.	**Procedure for biochemical kinase assay**	**18**
4.	**Screening of cytotoxic activity against a panel of sixty human tumor cell lines**	**19**
5.	**Analysis of cell cycle distribution**	**21**
6.	**Apoptosis assay**	**21**
7.	**Wound healing assay**	**22**
8.	**Docking of the co-crystalized ligands and 8c in the binding site of VEGFR-2 and FGFR-1**	**22**
9.	**Bioavailability radar chart for 8a-o from Swiss ADME free webtool**	**25**

1. NMR Spectra of target benzimidazole-dioxo(benzo)isoindoline hybrids 8a-o

2-(4-Chlorophenyl)-*N*-(1,3-dioxoisoindolin-2-yl)-1*H*-benzo[*d*]imidazole-5-carboxamide (**8a**)

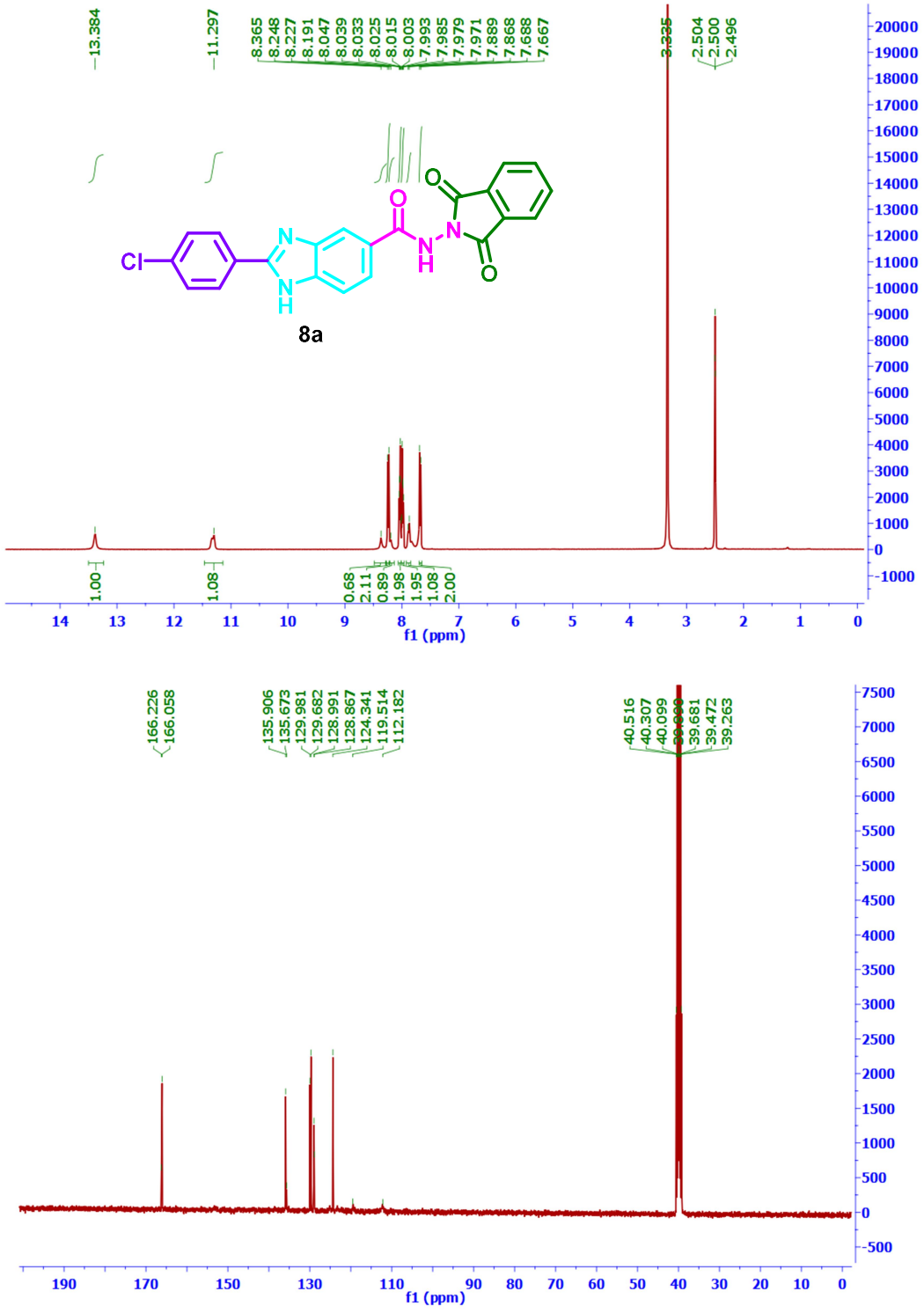

Figure 1. ^{1}H (400 MHz) and ^{13}C (100 MHz) NMR spectra of **8a** in DMSO-d_6

N-(1,3-Dioxoisoindolin-2-yl)-2-(3-methoxyphenyl)-1*H*-benzo[*d*]imidazole-5-carboxamide (**8b**)

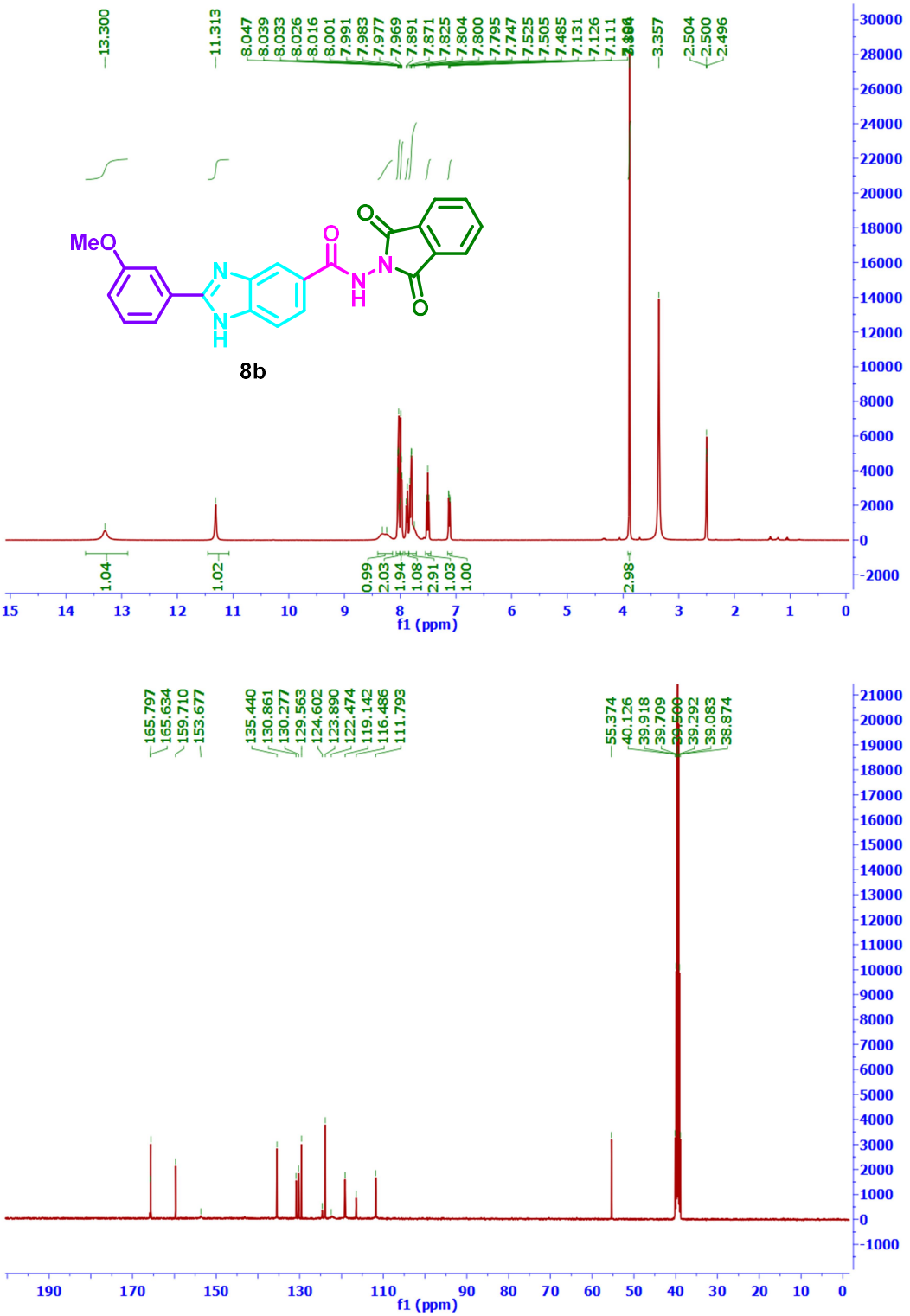

Figure 2. ^{1}H (400 MHz) and ^{13}C (100 MHz) NMR spectra of **8b** in DMSO-d_6

N-(1,3-Dioxoisoindolin-2-yl)-2-(4-methoxyphenyl)-1*H*-benzo[*d*]imidazole-5-carboxamide (**8c**)

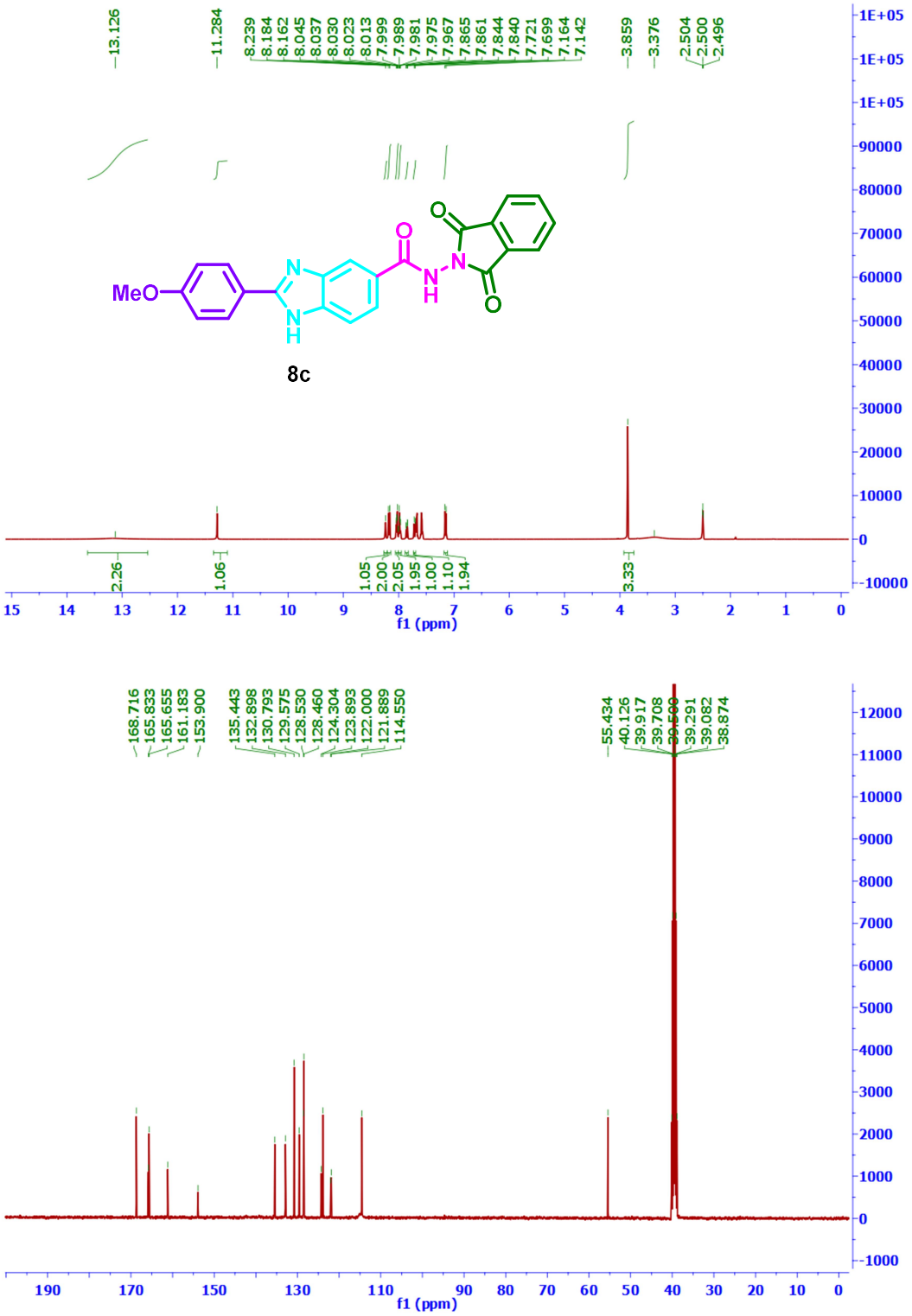

Figure 3. ^{1}H (400 MHz) and ^{13}C (100 MHz) NMR spectra of **8c** in DMSO-d_6

2-(2,5-Dimethoxyphenyl)-*N*-(1,3-dioxoisoindolin-2-yl)-1*H*-benzo[*d*]imidazole-5-carboxamide (**8d**)

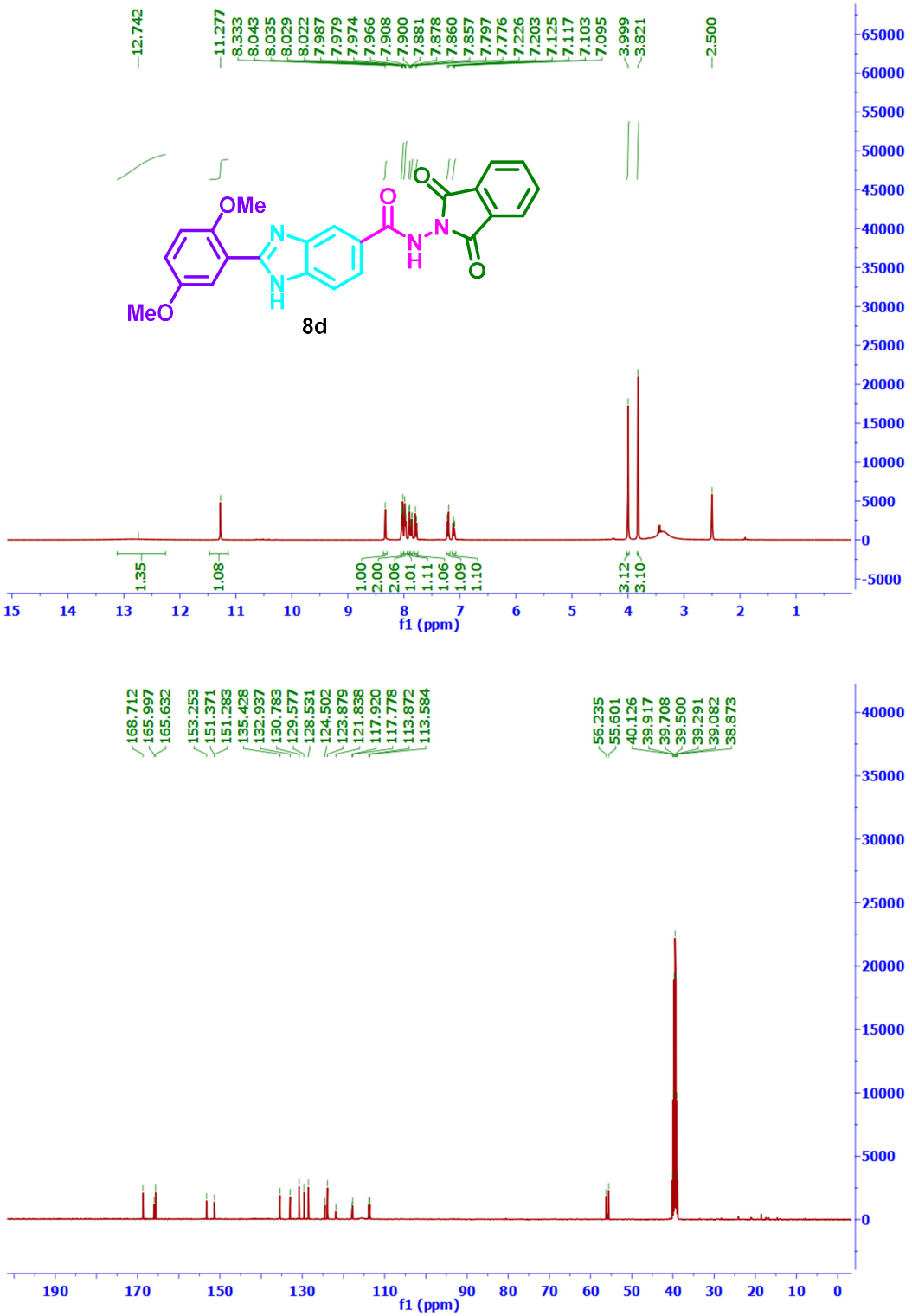

Figure 4. ^{1}H (400 MHz) and ^{13}C (100 MHz) NMR spectra of **8d** in DMSO-d_6

N-(1,3-Dioxoisoindolin-2-yl)-2-(3,4,5-trimethoxyphenyl)-1*H*-benzo[*d*]imidazole-5-carboxamide (**8e**)

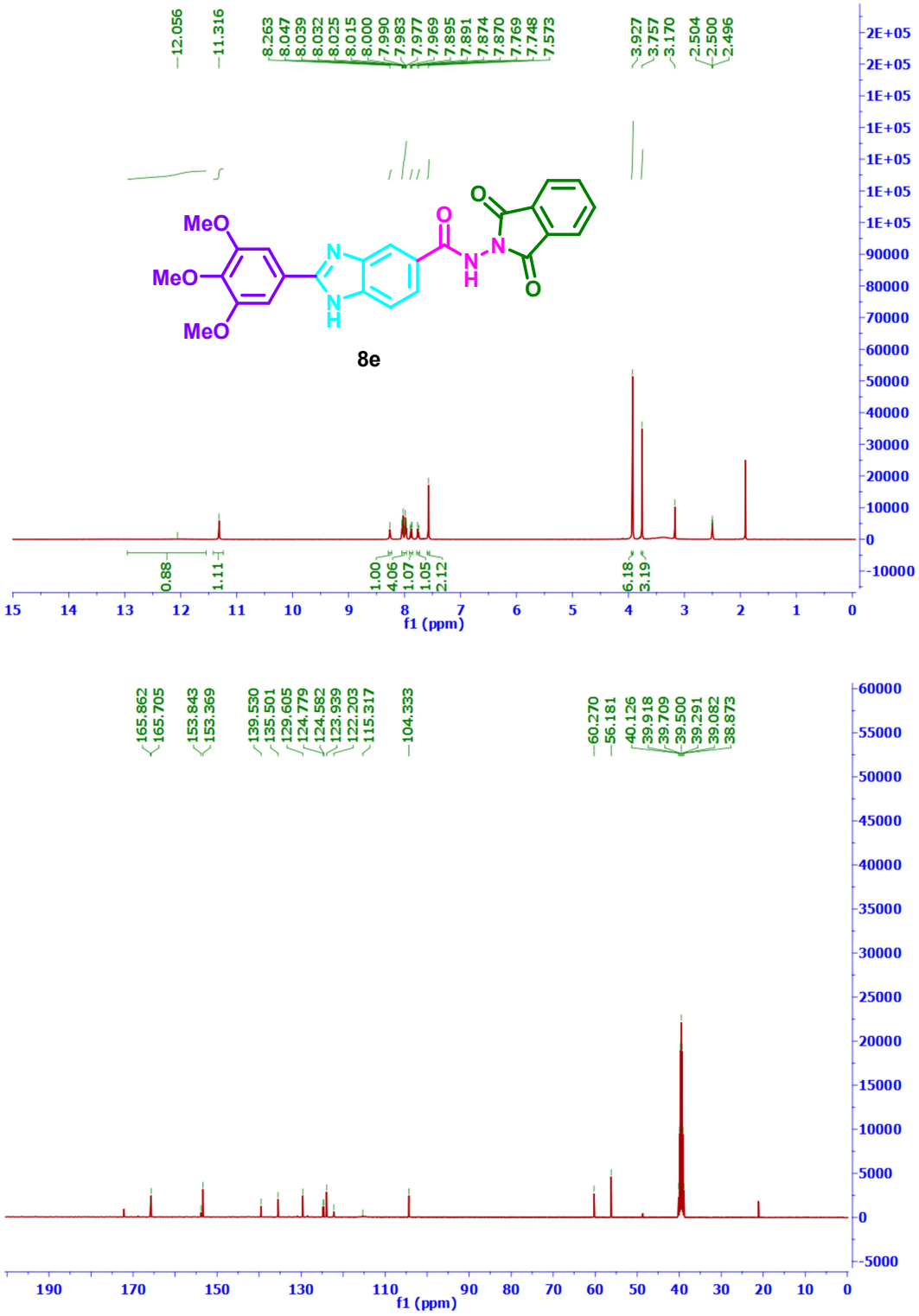

Figure 5. ^{1}H (400 MHz) and ^{13}C (100 MHz) NMR spectra of **8e** in DMSO-d_6

2-(2-(4-Chlorophenyl)-1*H*-benzo[*d*]imidazole-5-carboxamido)-1,3-dioxoisoindoline-5-carboxylic acid (**8f**)

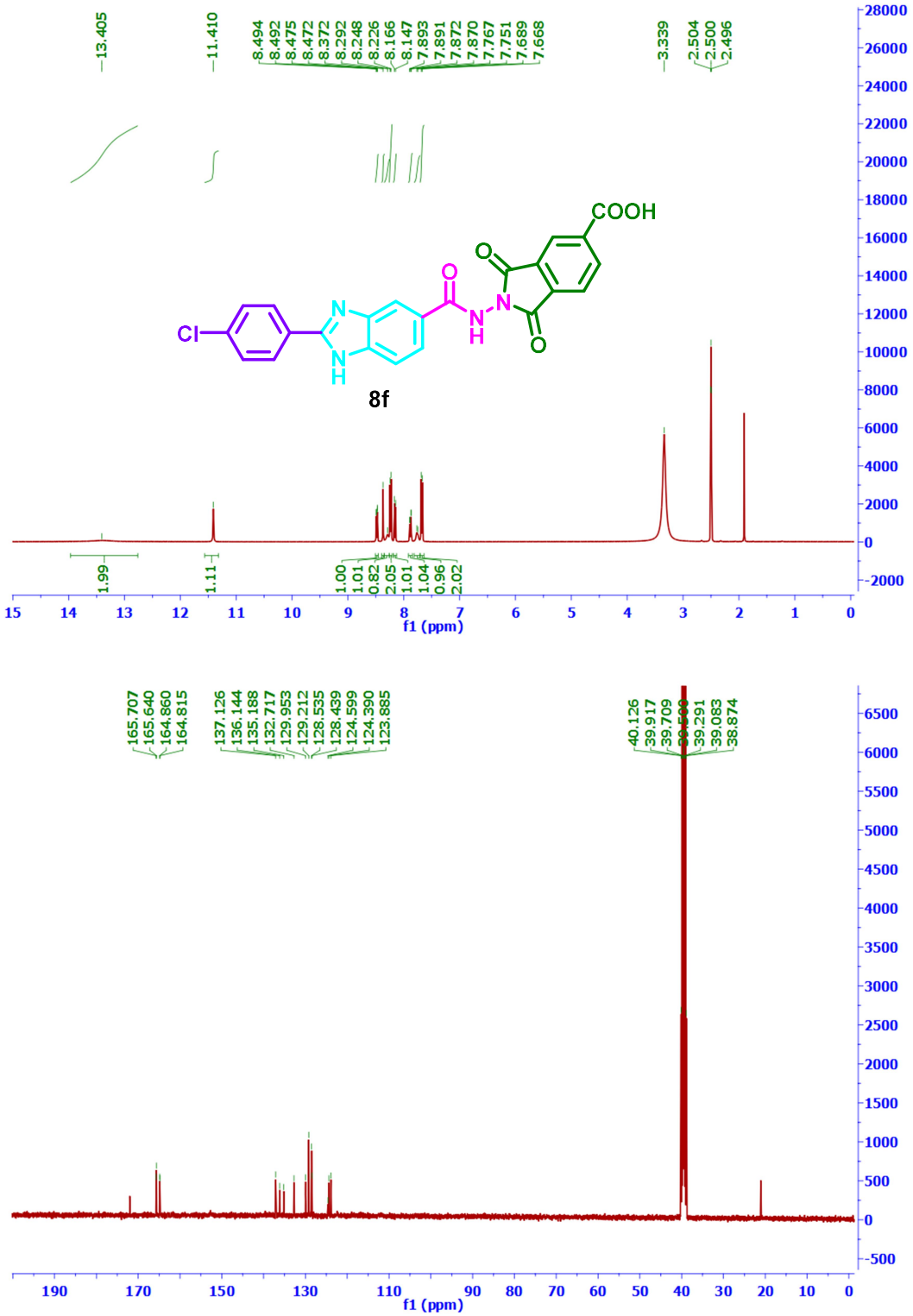

Figure 6. ^{1}H (400 MHz) and ^{13}C (100 MHz) NMR spectra of **8f** in DMSO-d_6

2-(2-(3-Methoxyphenyl)-1*H*-benzo[*d*]imidazole-5-carboxamido)-1,3-dioxoisoindoline-5-carboxylic acid (**8g**)

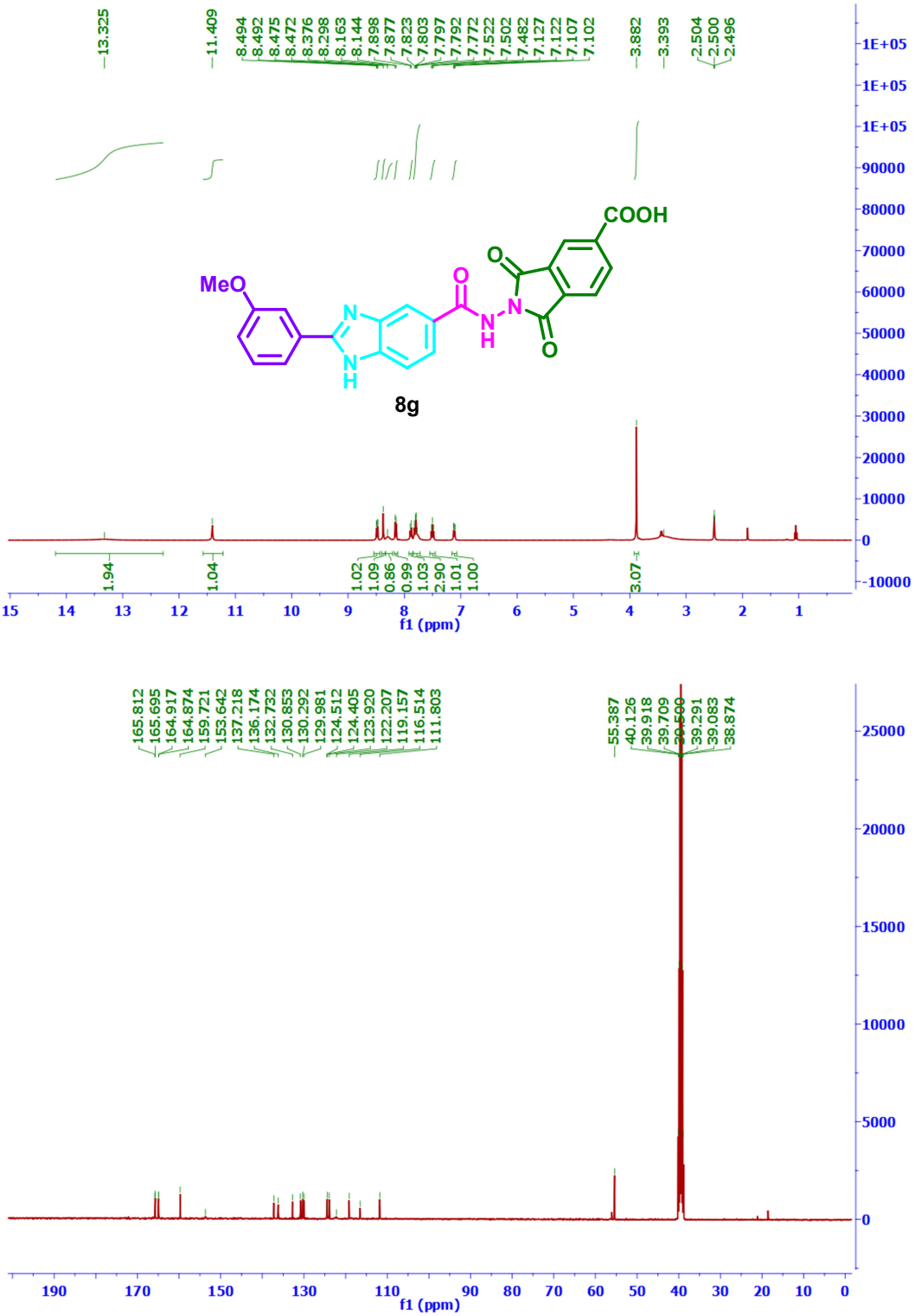

Figure 7. ^{1}H (400 MHz) and ^{13}C (100 MHz) NMR spectra of **8g** in DMSO-d_6

2-(2-(4-Methoxyphenyl)-1*H*-benzo[*d*]imidazole-5-carboxamido)-1,3-dioxoisoindoline-5-carboxylic acid (**8h**)

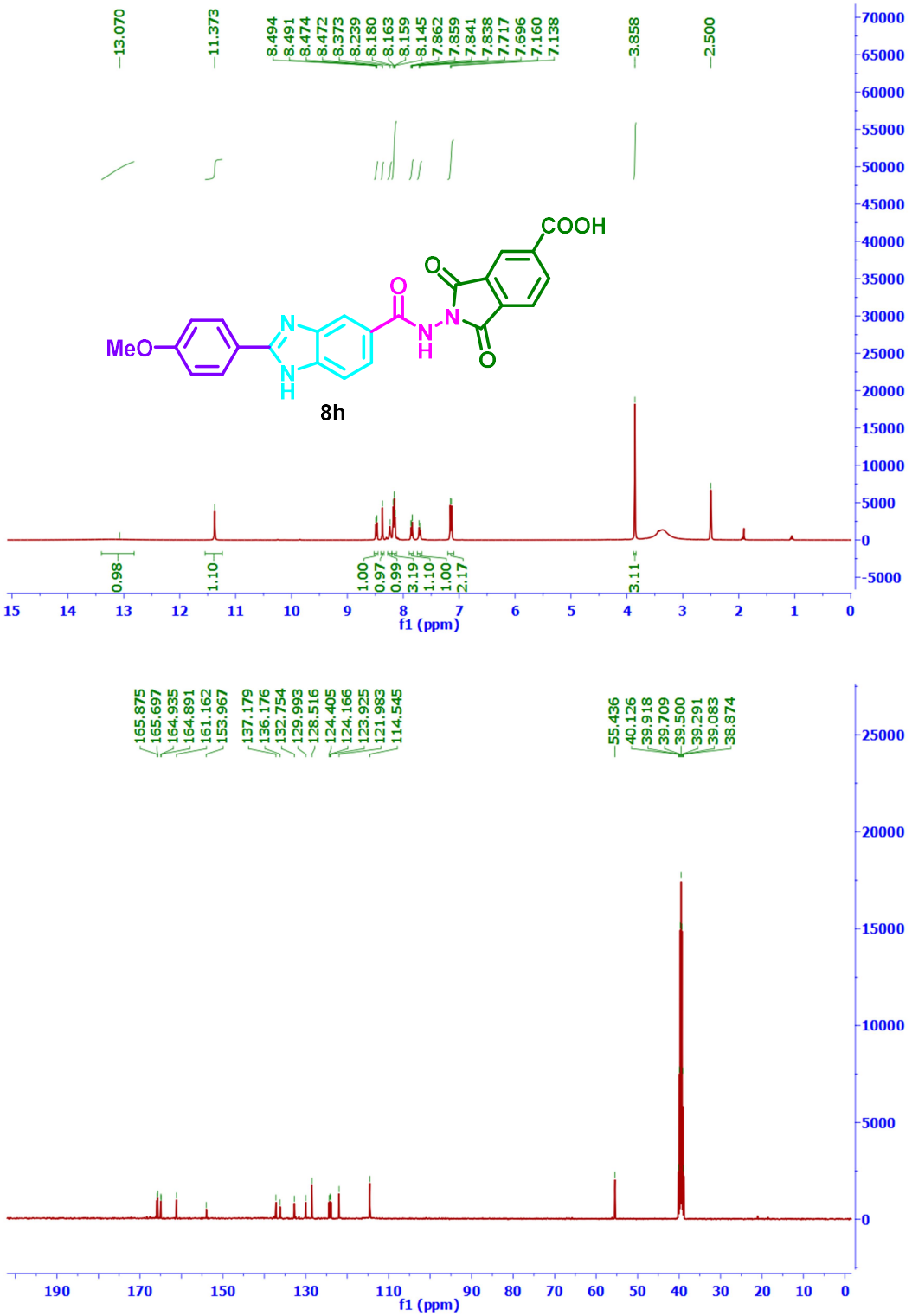

Figure 8. ^{1}H (400 MHz) and ^{13}C (100 MHz) NMR spectra of **8h** in DMSO-d_6

2-(2-(2,5-Dimethoxyphenyl)-1*H*-benzo[*d*]imidazole-5-carboxamido)-1,3-dioxoisoindoline-5-carboxylic acid (**8i**)

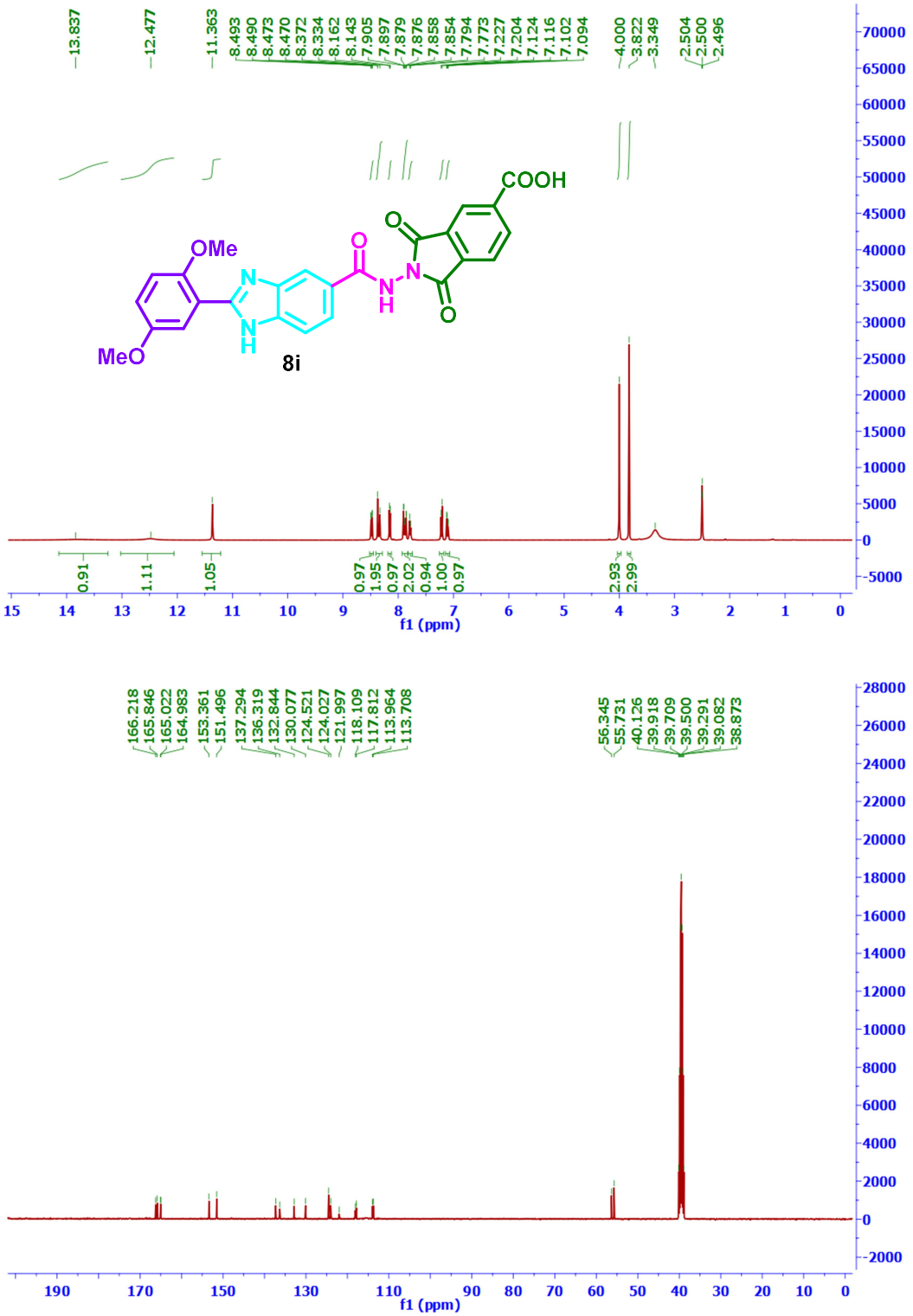

Figure 9. ^{1}H (400 MHz) and ^{13}C (100 MHz) NMR spectra of **8i** in DMSO-d_6

1,3-Dioxo-2-(2-(3,4,5-trimethoxyphenyl)-1*H*-benzo[*d*]imidazole-5-carboxamido)isoindoline-5-carboxylic acid (**8j**)

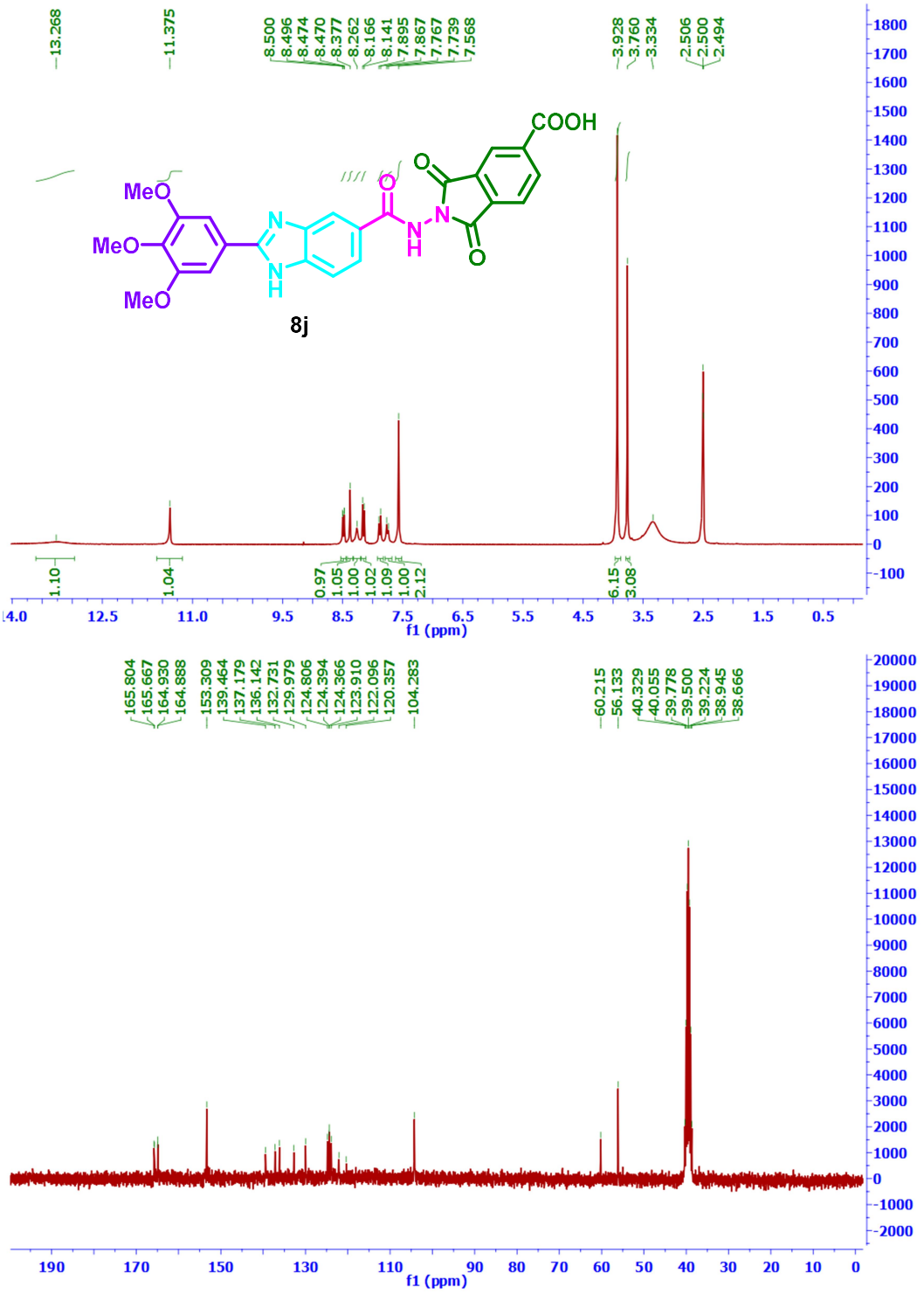

Figure 10. ^{1}H (400 MHz) and ^{13}C (100 MHz) NMR spectra of **8j** in DMSO-d_6

2-(4-Chlorophenyl)-*N*-(1,3-dioxo-1,3-dihydro-2*H*-benzo[*f*]isoindol-2-yl)-1*H*-benzo[*d*]imidazole-5-carboxamide (**8k**)

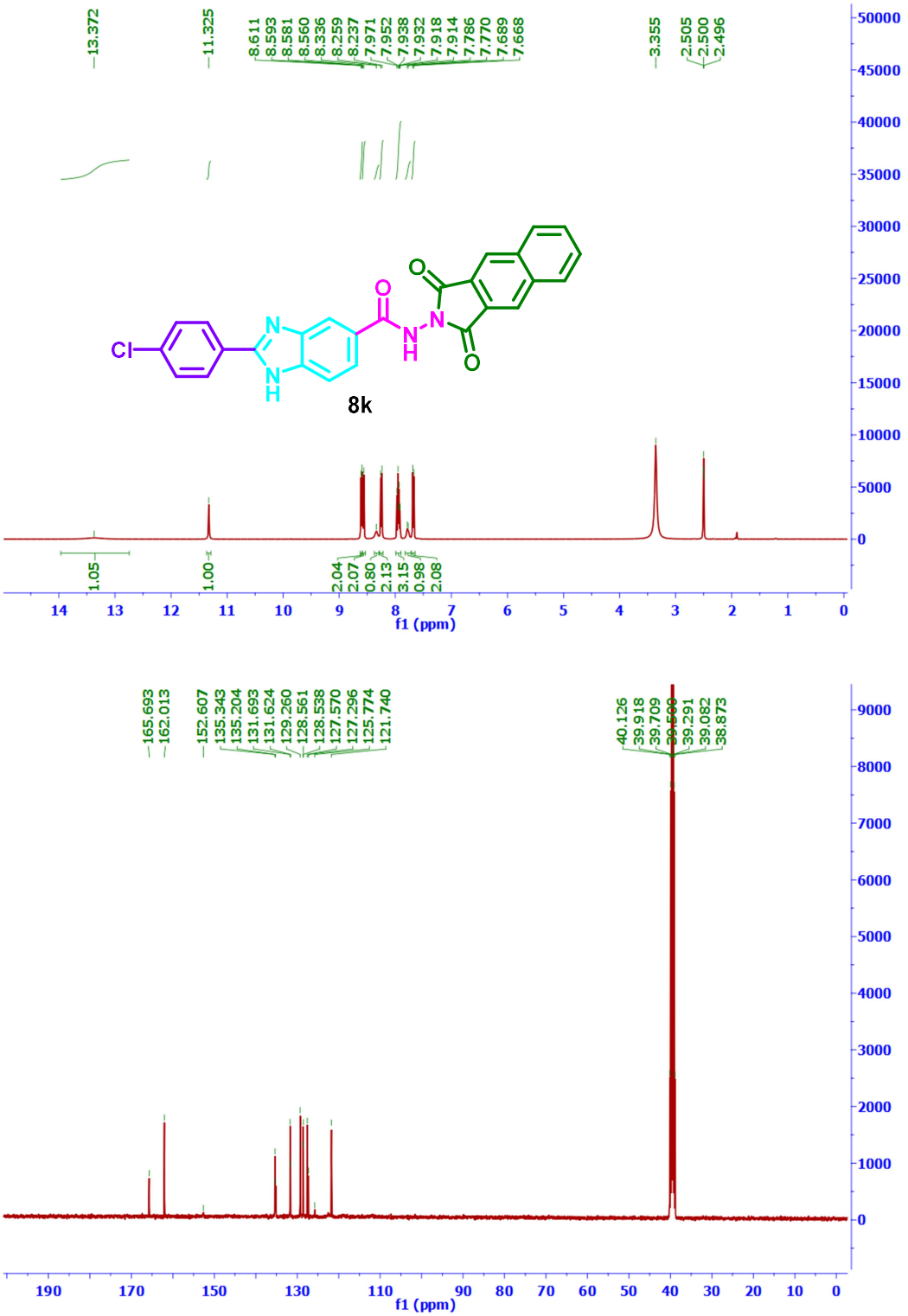

Figure 11. ^{1}H (400 MHz) and ^{13}C (100 MHz) NMR spectra of **8k** in DMSO-d_6

N-(1,3-Dioxo-1,3-dihydro-2*H*-benzo[*f*]isoindol-2-yl)-2-(3-methoxyphenyl)-1*H*-benzo[*d*]imidazole-5-carboxamide (**8l**)

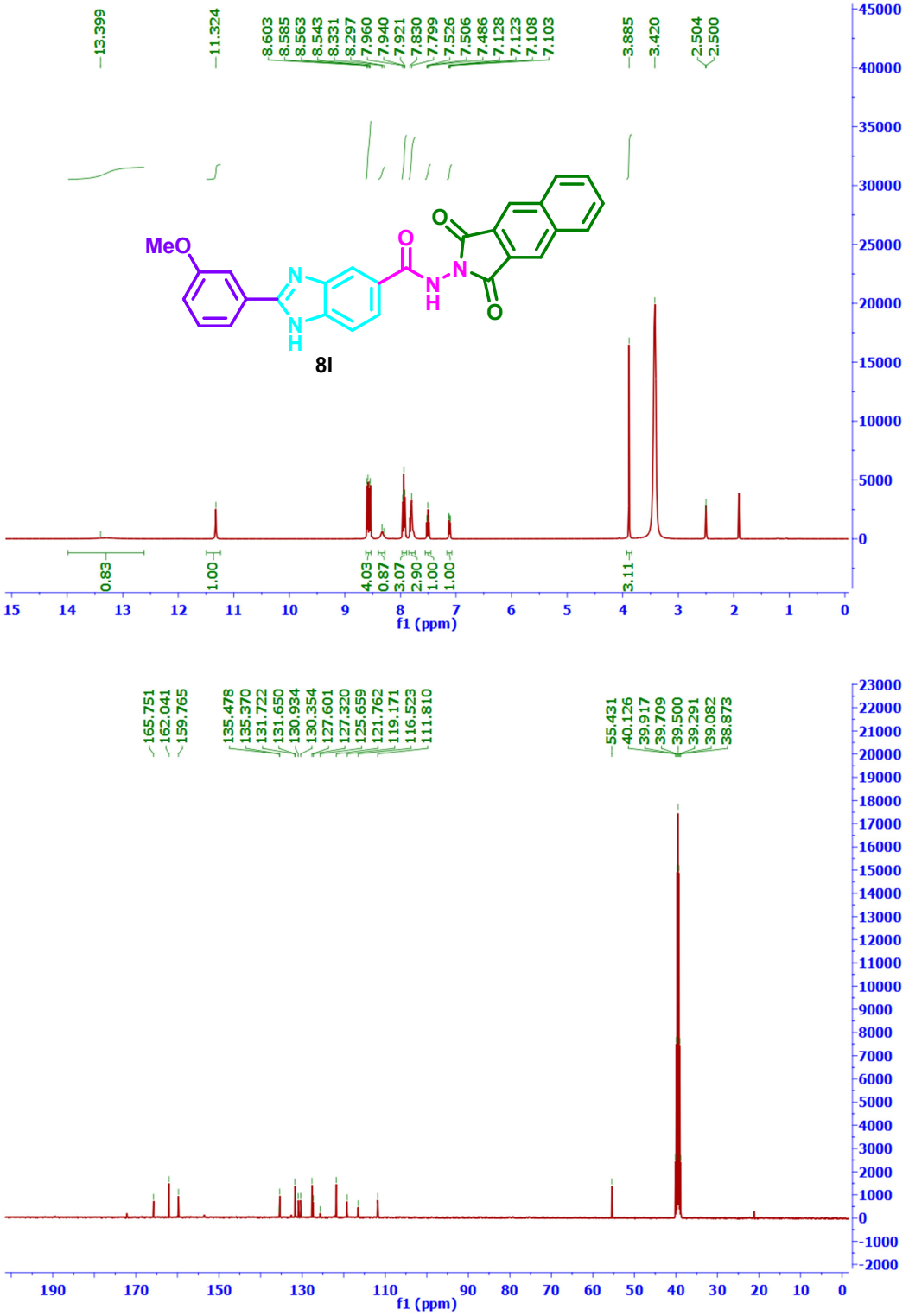

Figure 12. ^{1}H (400 MHz) and ^{13}C (100 MHz) NMR spectra of **8l** in DMSO-d_6

N-(1,3-Dioxo-1,3-dihydro-2*H*-benzo[*f*]isoindol-2-yl)-2-(4-methoxyphenyl)-1*H*-benzo[*d*]imidazole-5-carboxamide (**8m**)

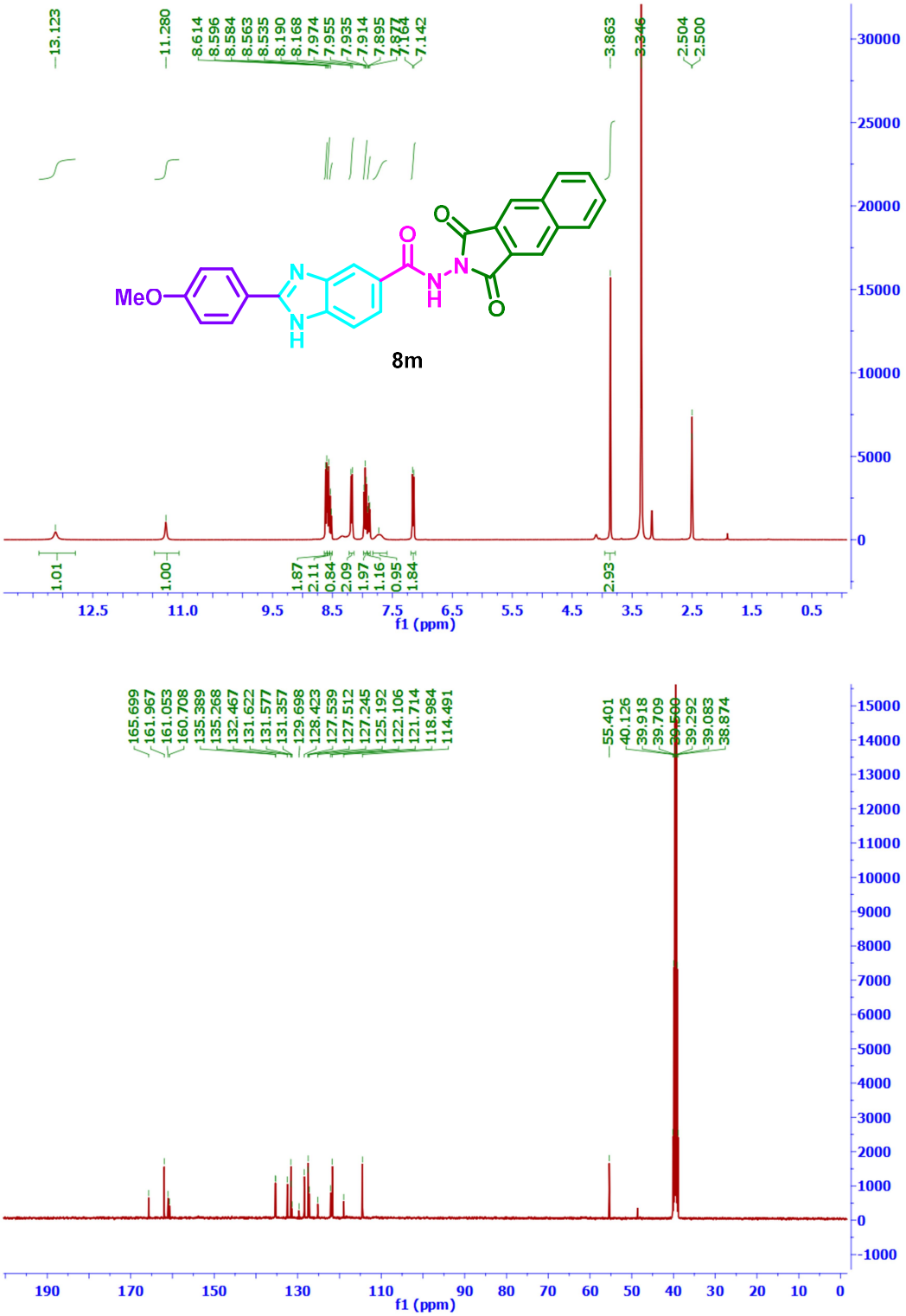

Figure 13. ^{1}H (400 MHz) and ^{13}C (100 MHz) NMR spectra of **8m** in DMSO-d_6

2-(2,5-Dimethoxyphenyl)-*N*-(1,3-dioxo-1,3-dihydro-2*H*-benzo[*f*]isoindol-2-yl)-1*H*-benzo[*d*]imidazole-5-carboxamide (**8n**)

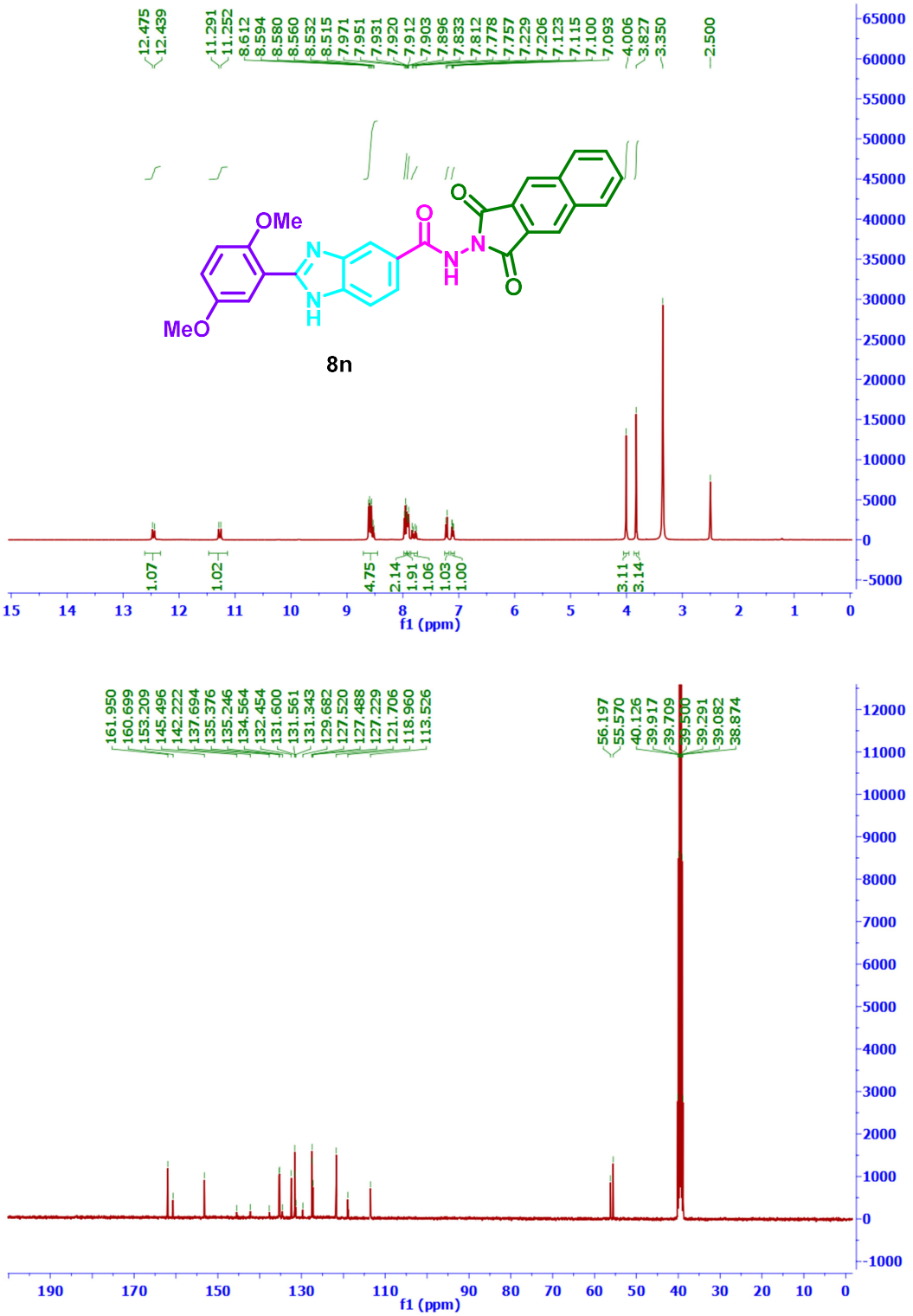

Figure 14. ^{1}H (400 MHz) and ^{13}C (100 MHz) NMR spectra of **8n** in DMSO-d_6

N-(1,3-Dioxo-1,3-dihydro-2*H*-benzo[*f*]isoindol-2-yl)-2-(3,4,5-trimethoxyphenyl)-1*H*-benzo[*d*]imidazole-5-carboxamide (**8o**)

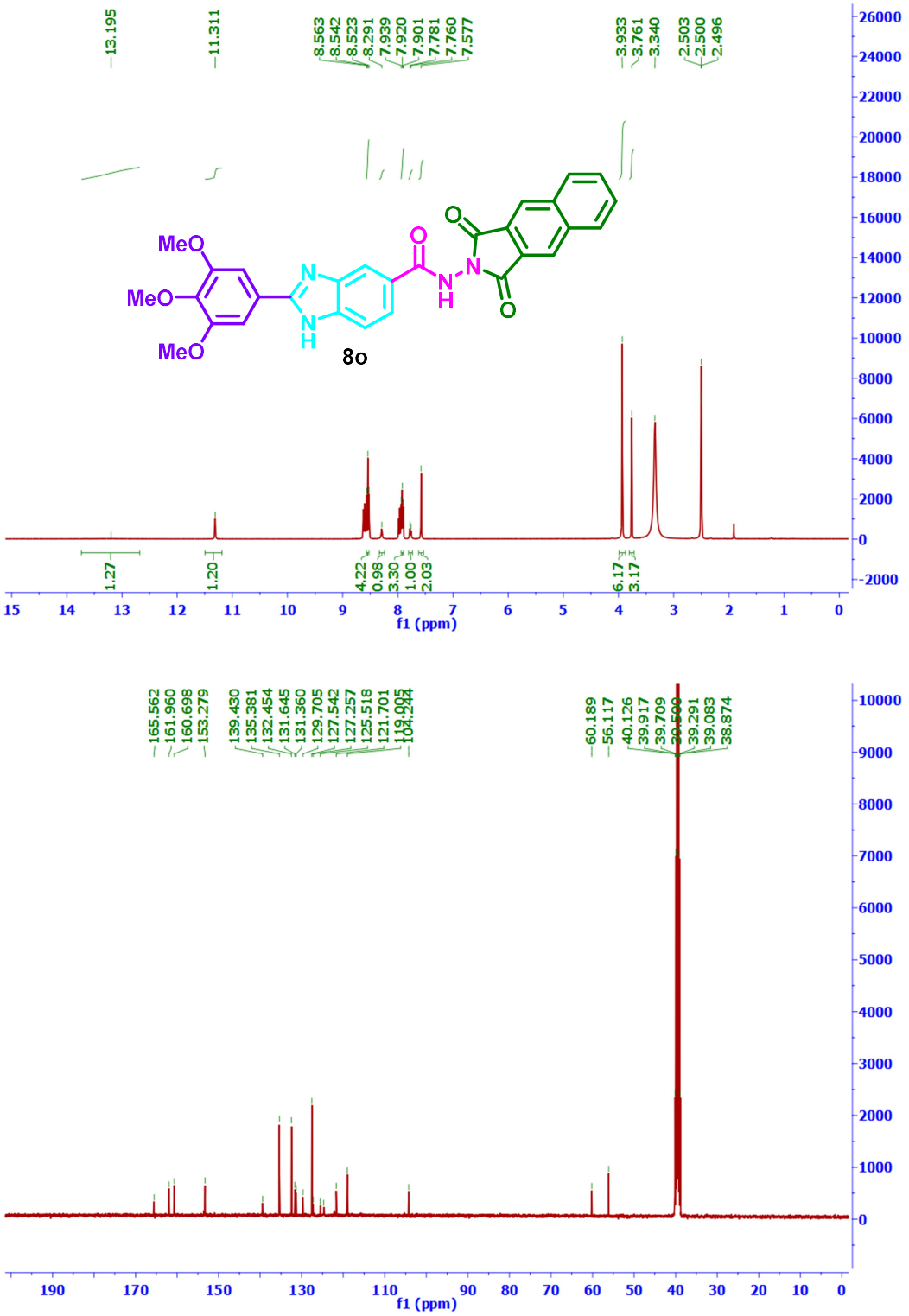

Figure 15. ^{1}H (400 MHz) and ^{13}C (100 MHz) NMR spectra of **8o** in DMSO-d_6

2. HRMS spectra of 8c and 8m

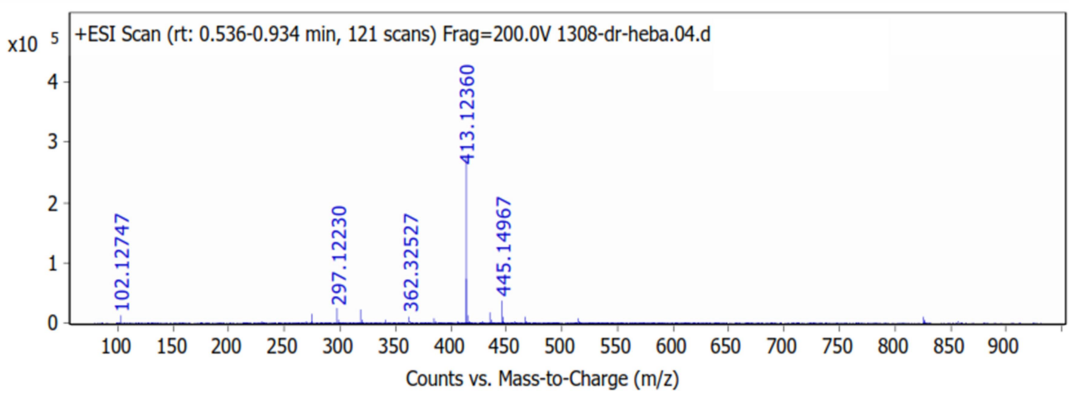

Figure 16. HRMS (+) ESI spectrum of **8c**

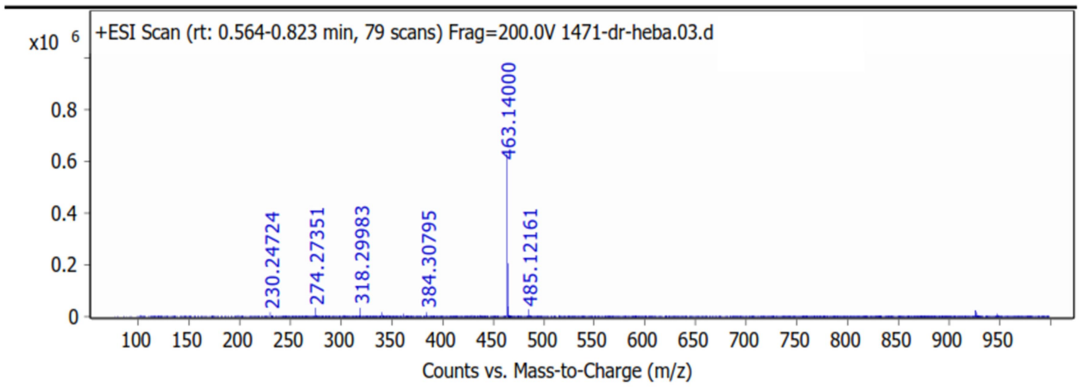

Figure 17. HRMS (+) ESI spectrum of **8m**

3. Procedure for biochemical kinase assay

The inhibitory activity against different kinases was determined using kinase kits (VEGFR-2 cat ID: 40325) and (FGFR-1 cat ID: 40210); purchased from BPS Biosciences and kinase-Glo Max luminescence kinase assay kit (Promega). Sorafenib was used as a reference multi-kinases inhibitor.

The assay was carried out according to the protocol provided by the manufacturer. A stock solution of the synthesized derivatives in 100% DMSO was prepared. Subsequently, the compounds were diluted to 10% DMSO.

A master mixture was prepared according to the number of wells. For VEGFR-2 and FGFR-1 biochemical assays each well include 6 µl of 5x Kinase Buffer 1 + 1 µl of 500 µM ATP + 1 µl of PTK Substrate (Poly-Glu,Tyr 4:1) (10 mg/ml) + 17 µl of distilled water. 1x Kinase buffer 1 was prepared by mixing 600 µl of 5x Kinase Buffer 1 with 2400 µl water to give 3 mL. Kinases were thawed on ice and were diluted with 1x Kinase Buffer 1.

To start the biochemical reaction, 25 µL of the master mixture was added to each well in 96 well plate. 5 µL of 10% DMSO was added to positive control wells and blank wells. 5 µL of diluted inhibitor was added to each well labelled with the test inhibitor so that the final concentration of DMSO is 1% in all reactions. Then 20 µL of (1 ng / µl) of VEGFR-2 or FGFR-1 in 1x kinase buffer was added to positive control wells and wells labelled with the inhibitor, while 20 µL 1x kinase buffer 1 was added to the blank wells.

The plate was incubated at 30 ^{o}C for 45 min. Subsequently, 50 µl of Kinase-Glo Max luminescence reagent was added to each well and the plate was covered with aluminum foil and incubated at room temperature for 15 min. Finally, the luminescence was recorded using multimode microplate reader. Kinase activity assays were performed in duplicate at each concentration.

The luminescence data were analyzed as follows. The difference between luminescence intensities in the absence of kinase (Lu_t) and in the presence of kinase (Lu_c) was defined as 100 % activity ($Lu_t - Lu_c$). Using luminescence signal (Lu) in the presence of the compound, % activity was calculated as: % activity = $\{(Lu_t - Lu)/(Lu_t - Lu_c)\} \times 100\%$.

4. Screening of cytotoxic activity against a panel of sixty human tumor cell lines

The selected compounds by NCI were evaluated for their anticancer activity in a two-stage process. First, these compounds were screened against the full NCI 60 cell lines panel at a single high dose of 10 μM. Then, the output from the single dose screen is reported as a mean graph. Second, compounds exhibiting significant growth inhibition were evaluated against the 60 cell panel at five different minimal concentrations.

Assay protocol. The human tumor cell lines of the cancer screening panel are grown in RPMI 1640 medium containing 5% fetal bovine serum and 2 mM L-glutamine. For a typical screening experiment, cells are inoculated into 96 well microtiter plates in 100 μL at plating densities ranging from 5000 to 40,000 cells/well depending on the doubling time of individual cell lines. After cell inoculation, the microtiter plates are incubated at 37 ^{o}C, 5% CO_2, 95% air and 100% relative humidity for 24 h prior to addition of the experimental drugs.

After 24h, two plates of each cell line are fixed in situ with TCA, to represent a measurement of the cell population for each cell line at the time of drug addition (Tz). The experimental drugs are solubilized in dimethyl sulfoxide at 400-fold the desired final maximum test concentration and stored frozen prior to use. At the time of drug addition, an aliquot of frozen concentrate is thawed and diluted to twice the desired final maximum test concentration with complete medium containing 50 μg/mL gentamicin. Additional four, 10-fold or ½ log serial dilutions are made to provide a total of five drug concentrations plus control.

Aliquots of 100 mL of these different drug dilutions are added to the appropriate microtiter wells already containing 100 mL of medium, resulting in the required final drug concentrations. Following drug addition, the plates are incubated for an additional 48 h at 37 ^{o}C, 5% CO_2, 95% air, and 100% relative humidity. For adherent cells, the assay is terminated by the addition of cold TCA. Cells are fixed in situ by the gentle addition of 50 μL of cold 50% (w/v) TCA (final concentration, 10% TCA) and incubated for 60 min at 4 ^{o}C. The supernatant is discarded, and the plates are washed five times with tap water and air dried. Sulforhodamine B (SRB) solution (100 mL) at 0.4% (w/v) in 1% acetic acid is added to each well, and plates are incubated for 10 min at room temperature. After staining, unbound dye is removed by washing five times with 1% acetic acid and the plates are air dried. Bound stain is subsequently solubilized with 10 mM trizma base, and the absorbance is read on an automated plate reader at a wavelength of 515 nm. For suspension cells, the methodology is the same except that the assay is terminated by fixing settled cells at the bottom of the wells by gently adding 50 μl of 80% TCA (final concentration, 16% TCA). Using the seven

absorbance measurements [time zero, (Tz), control growth, (C), and test growth in the presence of drug at the five concentration levels (Ti)], the percentage growth is calculated at each of the drug concentrations levels.

Percentage growth inhibition is calculated as: [(Ti Tz)/(C–Tz)] x 100 for concentrations for which Ti>/=Tz and [(Ti-Tz)/Tz] x 100 for concentrations for which Ti < Tz.

Three dose response parameters are calculated for each experimental agent. Growth inhibition of 50% (GI_{50}) is calculated from [(Ti -Tz)/(C–Tz)] x 100 = 50, which is the drug concentration resulting in a 50% reduction in the net protein increase (as measured by SRB staining) in control cells during the drug incubation. The drug concentration resulting in total growth inhibition (TGI) is calculated from Ti = Tz. The LC_{50} (concentration of drug resulting in a 50% reduction in the measured protein at the end of the drug treatment as compared to that at the beginning) indicating a net loss of cells following treatment is calculated from [(Ti–Tz)/Tz] x 100 = ⁻50. Values are calculated for each of these three parameters if the level of activity is reached; however, if the effect is not reached or is exceeded, the value for that parameter is expressed as greater or less than the maximum or minimum concentration tested. Results for each compound were reported as a mean graph of the percent growth of the treated cells when compared to the untreated control cells. There after obtaining the results for one dose assay, analysis of historical Development Therapeutics Programme (DTP) was performed and compounds which satisfies predetermined threshold inhibition criteria is selected for NCI full panel 5 dose assay.

5. Analysis of Cell Cycle Distribution

MCF-7: Breast Cancer was obtained from Nawah Scientific Inc., (Mokatam, Cairo, Egypt). Cells were maintained in DMEM media supplemented with 100 mg/mL of streptomycin, 100 units/mL of penicillin and 10% of heat-inactivated fetal bovine serum in humidified, 5% (v/v) CO_2 atmosphere at 37 °C. After treatment with test compound **8m** for 48h, cells (105 cells) are collected by trypsinization and washed twice with ice-cold PBS (pH 7.4). Cells are re-suspended in two milliliters of 60% ice-cold ethanol and incubated at 4ºC for 1h for fixation. Fixed cells are washed twice again with PBS (pH 7.4) and re-suspended in 1 mL of PBS containing 50 µg/mL RNAase A and 10 µg/mL propidium iodide (PI). After 20 min of incubation in dark at 37 ^{o}C, cells are analyzed for DNA contents using flow cytometry analysis using FL2 (λex/em 535/617 nm) signal detector (ACEA Novocyte™ flowcytometer, ACEA Biosciences Inc., San Diego, CA, USA). For each sample, 12,000 events are acquired. Cell cycle distribution is calculated using ACEA NovoExpress™ software (ACEA Biosciences Inc., San Diego, CA, USA).

6. Apoptosis assay

Apoptosis and necrosis cell populations are determined using Annexin V-FITC apoptosis detection kit (Abcam Inc., Cambridge Science Park, Cambridge, UK) coupled with 2 fluorescent channels flowcytometry. After treatment with test compounds for 48h, cells (105 cells) are collected by trypsinization and washed twice with ice-cold PBS (pH 7.4). Then, cells are incubated in dark with 0.5 ml of Annexin V-FITC/PI solution for 30 min in dark at room temperature according to manufacturer protocol. After staining, cells are injected via ACEA Novocyte™ flowcytometer (ACEA Biosciences Inc., San Diego, CA, USA) and analysed for FITC and PI fluorescent signals using FL1 and FL2 signal detector, respectively (λex/em 488/530 nm for FITC and λex/em 535/617 nm for PI). For each sample, 12,000 events are acquired and positive FITC and/or PI cells are quantified by quadrant analysis and calculated using ACEA NovoExpress™ software (ACEA Biosciences Inc., San Diego, CA,
USA).

7. Wound healing assays

Cells were plated at density $2x10^5$ /well onto a coated 12-well plate for scratch wound assay and cultured overnight in 5% FBS-DMEM at 37 °C and 5% CO_2. On the next day, horizontal scratches were introduced into the confluent monolayer; the plate was washed thoroughly with PBS, control wells were replenished with fresh medium while drug wells were treated with fresh media containing drug. Images were taken using an inverted microscope at the indicated time intervals. The plate was incubated at 37 °C and 5% CO_2 in-between time points. The acquired images are displayed below and were analyzed by MII ImageView software version 3.7.

8. Docking in the binding sites' of VEGFR-2 and FGFR-1

Docking experiments were performed on Autodock Vina software (Trott, O., Olson, A.J., 2010. AutoDock Vina: improving the speed and accuracy of docking with a new scoring function, efficient optimization, and multithreading. J. Comput. Chem. 31, 455–461. https://doi.org/10.1002/jcc.21334). Briefly, the crystal structure of VEGFR-2 (PDB ID: 4ASD) and FGFR-1 (PDB ID: 4V01) were downloaded from the protein data bank. Initially the proteins were prepared for the intended docking study by removal of water molecules followed by protonation, adjustment of partial charges and the receptor was saved in pdbqt format. The co-crystalized ligand and **8c** and **8m** were prepared and also saved in pdbqt format. Self-docking of the co-crystalized ligand was performed to validate the docking protocol. After validation experiments (**Figures 18** and **19**), **8c** and **8m** were docked in the binding sites of both enzymes and the binding free energy was detected and 3D poses was visualized by free BIOVIA discovery visualizer 2021 (https://discover.3ds.com/discovery-studio-visualizer) (**Figures 20** and **21**).

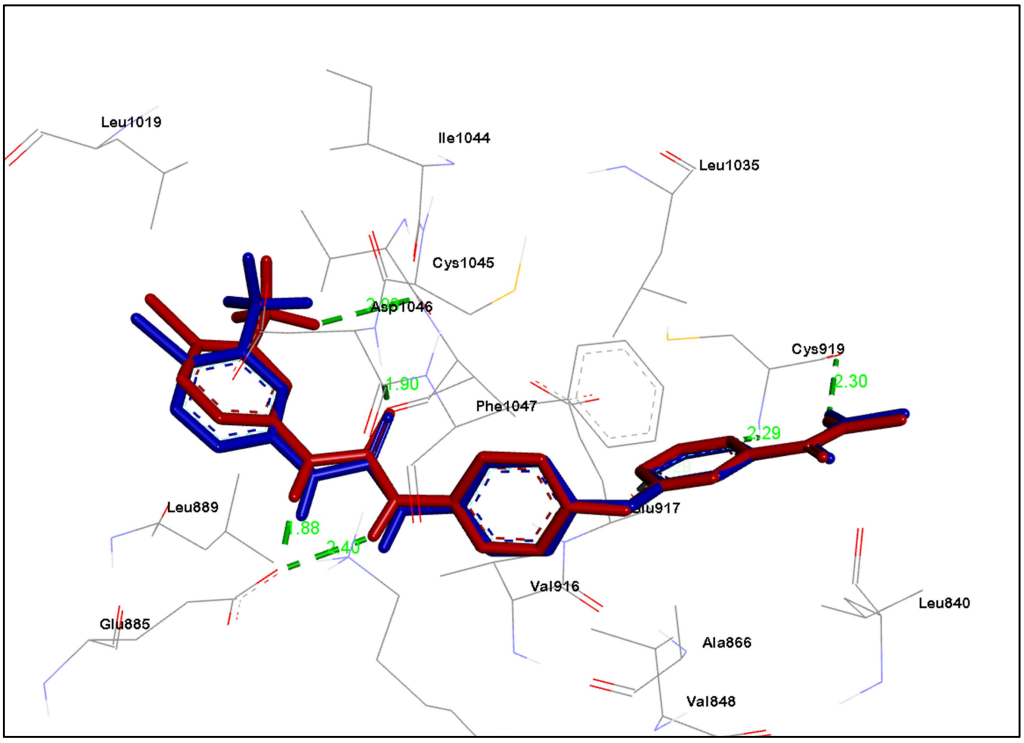

Figure 18. 3D diagram of the overlay of docked pose (red) and the co-crystallized ligand (blue) in the VEGFR-2 active site

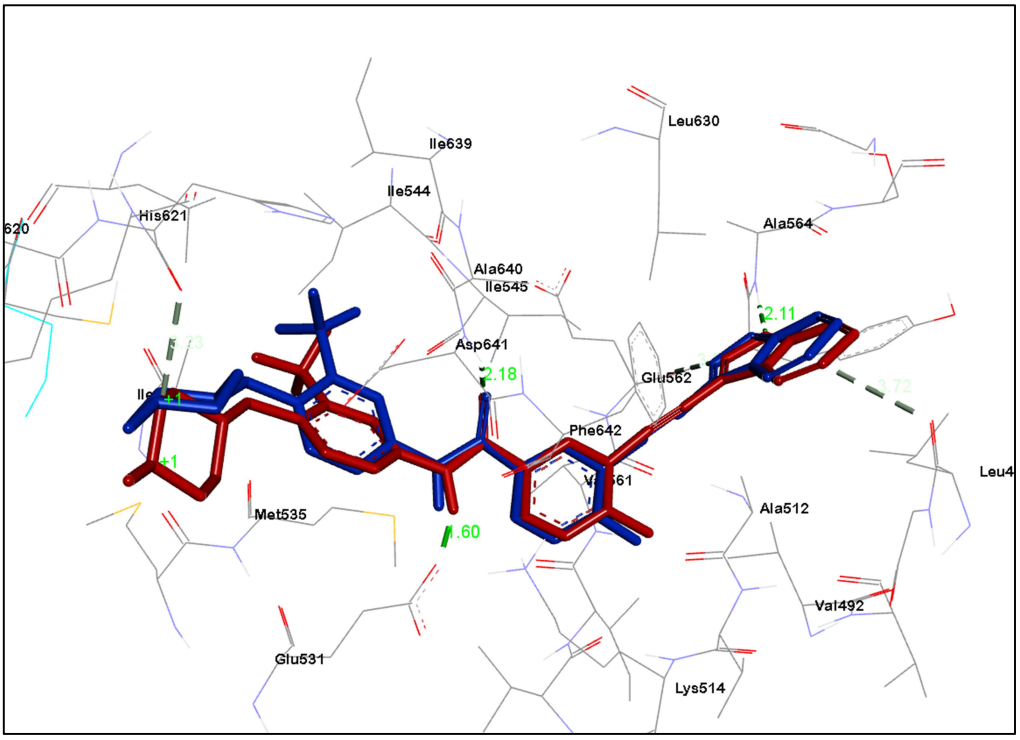

Figure 19. 3D diagram of the overlay of the docked pose (red) and the co-crystallized ligand (blue) in the FGFR-1 active site

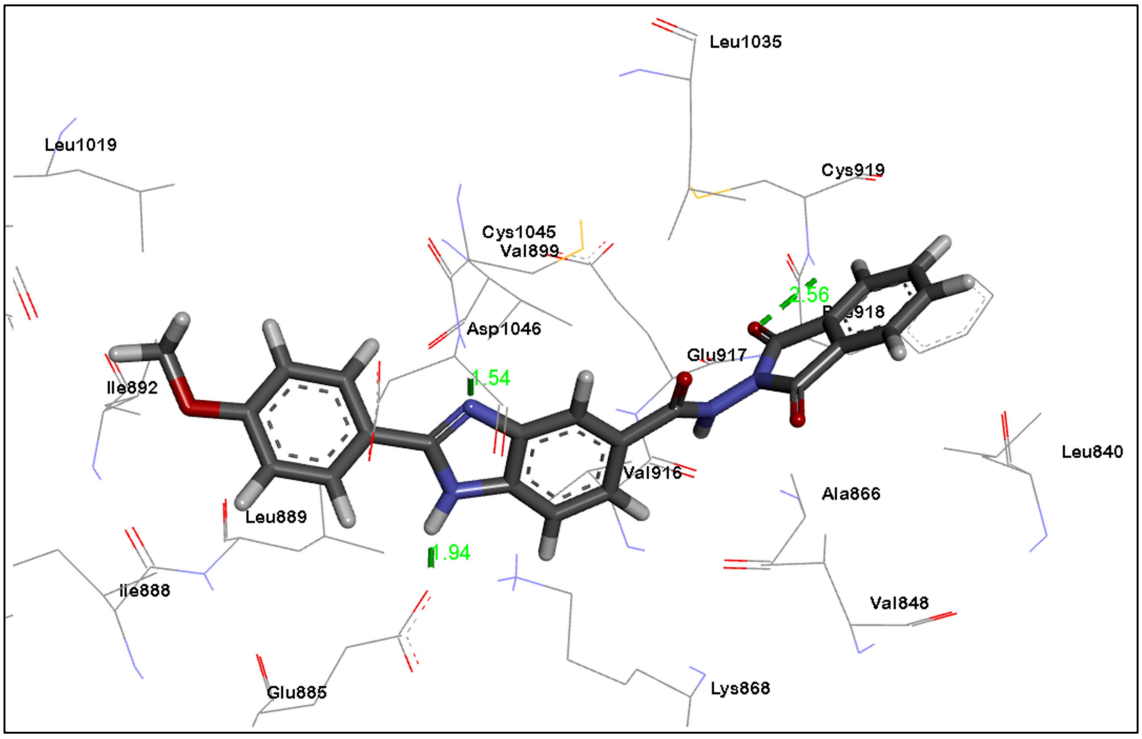

Figure 20. 3D presentation of **8c** in the binding site of VEGFR-2

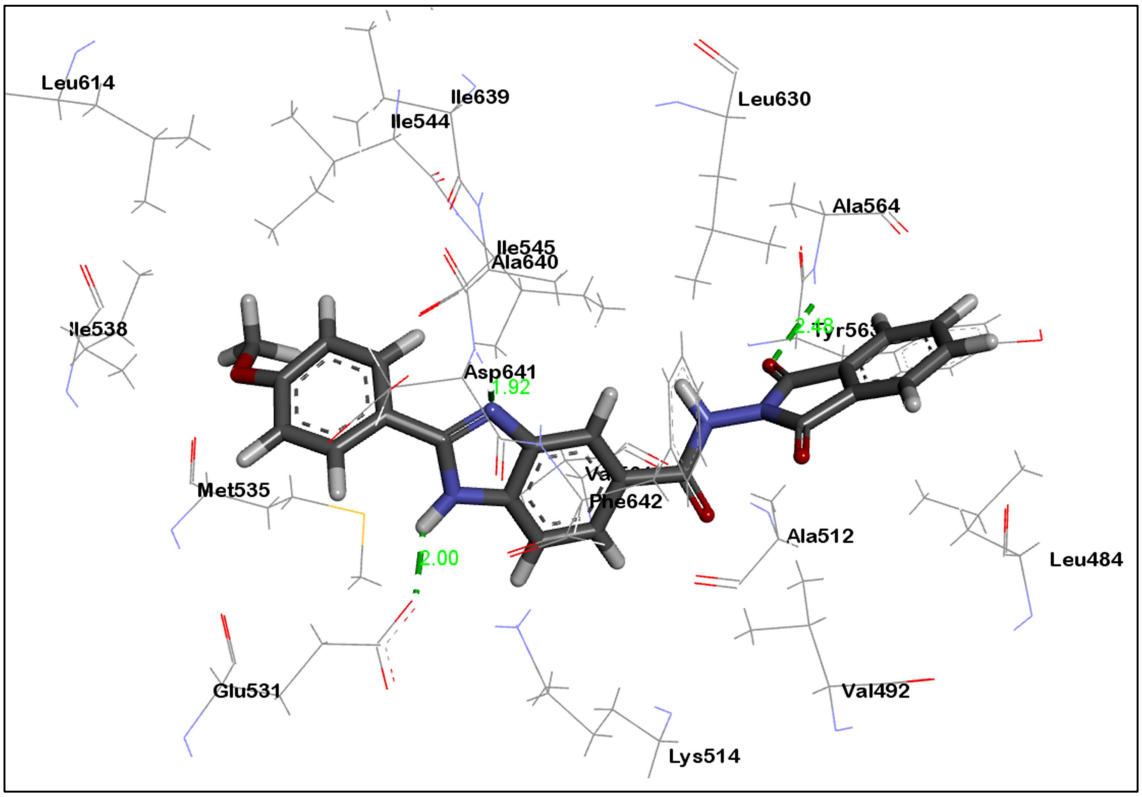

Figure 21. 3D presentation of **8c** in the binding site of FGFR-1

9. Bioavailability radar chart for 8a-o from SwissADME free webtool

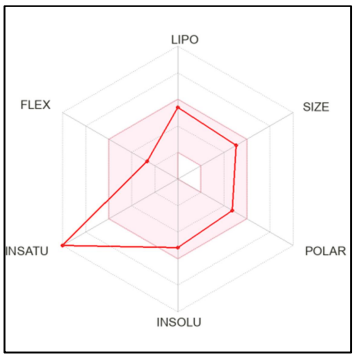

8a

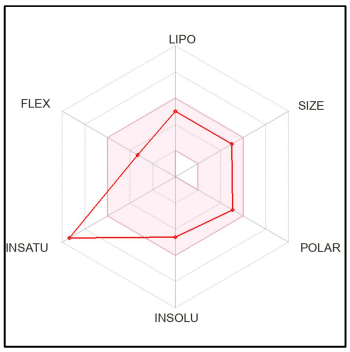

8b

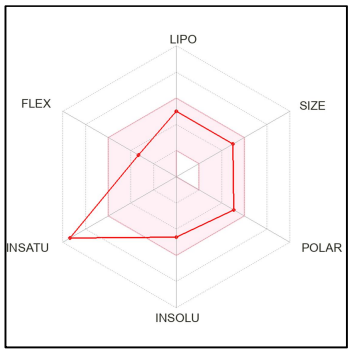

8c

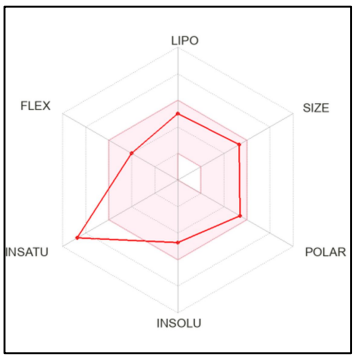

8d

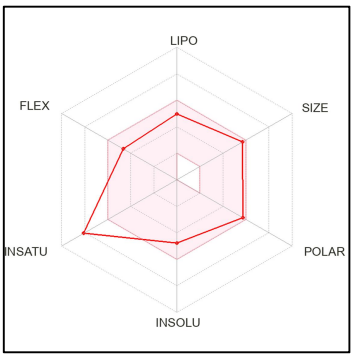

8e

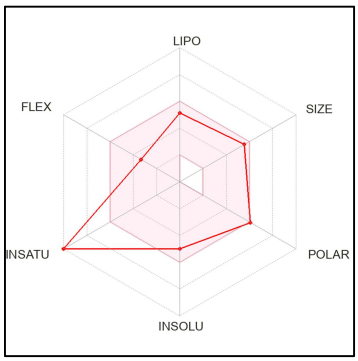

8f

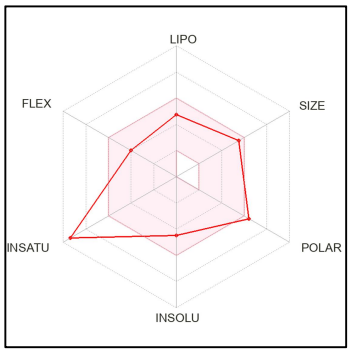

8g

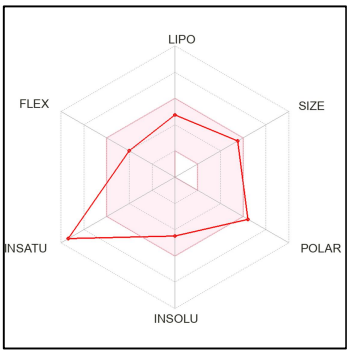

8h

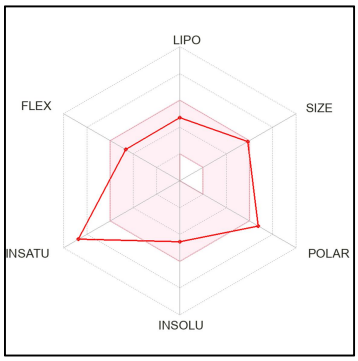

8i

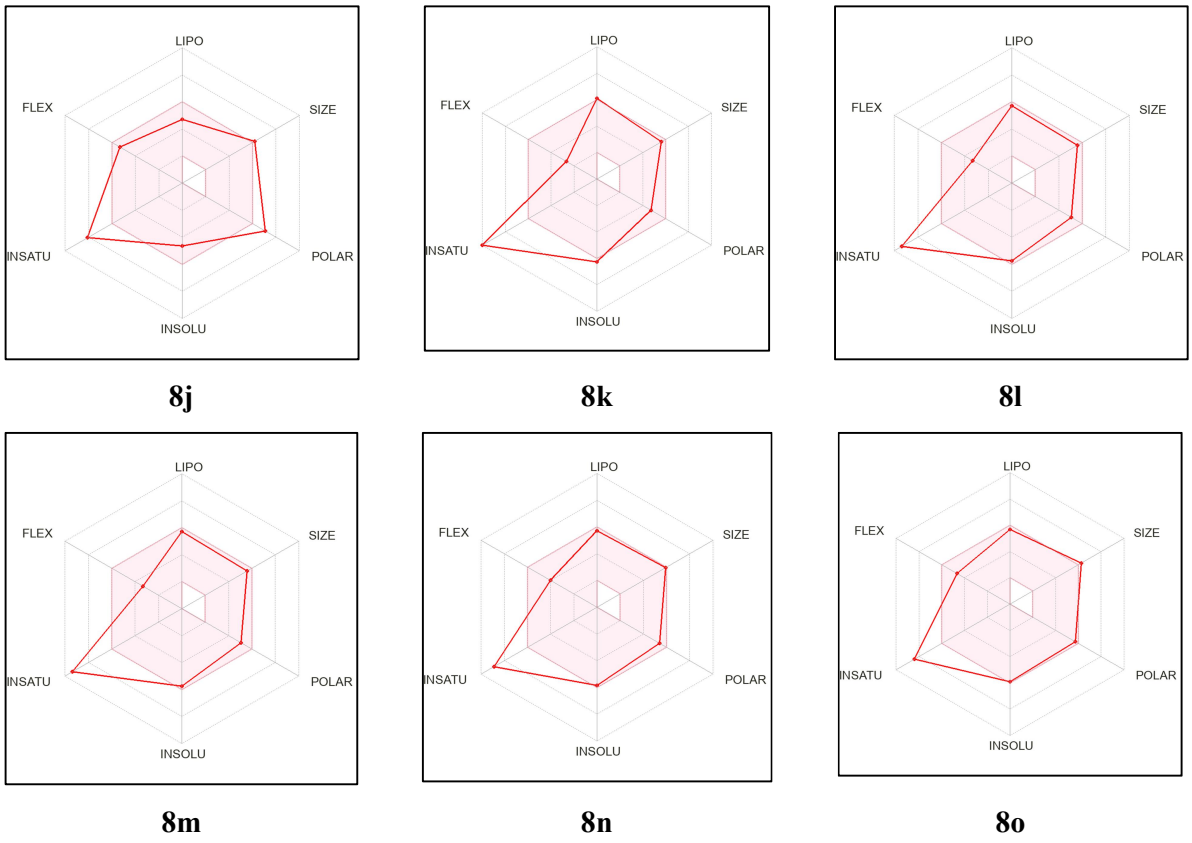

Figure 22. Bioavailability radar chart for **8a-o**